Electronic and vibrational excitation of single molecules with a scanning tunneling microscope

2 **AUTHORS**, INCLUDING:

Lincoln J Lauhon
Northwestern University

181 PUBLICATIONS **10,636** CITATIONS

ELSEVIER

Electronic and vibrational excitation of single molecules with a scanning tunneling microscope

L.J. Lauhon, W. Ho *

Laboratory of Atomic and Solid State Physics and Cornell Center for Materials Research, Cornell University, Ithaca, NY 14853, USA

Abstract

The electronic and vibrational excitations of single acetylene, pyridine, and benzene molecules on Cu(001) were studied by scanning tunneling microscopy at 9 K. Electrons of 0–5 eV were used to induce dissociation, desorption, diffusion, rotation, and vibrational excitation of these molecules. The dissociation products were characterized by imaging, single molecule vibrational spectroscopy, and rotational excitation. The STM is shown to be a very versatile tool for inducing a molecule to explore its excited state potential energy surface and describing the possible results. © 2000 Elsevier Science B.V. All rights reserved.

Keywords: Alkynes; Aromatics; Copper; Scanning tunneling microscopy; Single crystal surfaces; Surface chemical reaction

1. Introduction

The scanning tunneling microscope (STM), in addition to producing informative images of surfaces decorated with atoms and molecules, can be used to deliver electrons of well-defined energy to an adsorbate positioned directly under the tip. We are interested in exploring the possible outcomes of the electronic excitation induced by such electrons. The phenomena to be described include dissociation, desorption, diffusion, rotation, and vibrational excitation. The molecules chosen for study are acetylene, benzene, pyridine, and their dissociation products adsorbed on the Cu(001) surface at 9 K.

Experiments were performed using a home-built variable-temperature STM housed in an ultra-high-vacuum chamber with a base pressure of

2×10^{-11} Torr [1]. The sample and tip preparation have been described previously [2]. Molecules were dosed to coverages of ~ 0.001 ML via a capillary array doser attached to a variable leak valve.

Acetylene (C_2H_2) adsorbs molecularly in the fourfold hollow site of the Cu(001) surface [3]. The C$-$H bonds bend away from the surface, and the molecular plane is perpendicular to the surface. Acetylene images as an elongated depression and is found in two equivalent orientations (Fig. 1a–c). Rotation between the two orientations may be induced by energetic electrons or thermal excitations. The barrier to rotation of 0.17 eV was determined by STM measurements of thermal rotation rates [4].

Low-energy electrons from the STM tip can be used to induce the dissociation of HCCH into CCH and CC in a controlled manner. The method used to control C$-$H bond scission was as follows. The tip was positioned above the center of the molecule and the feedback turned off. The tip was

---

* Corresponding author. Fax: +1-607-255-6428.

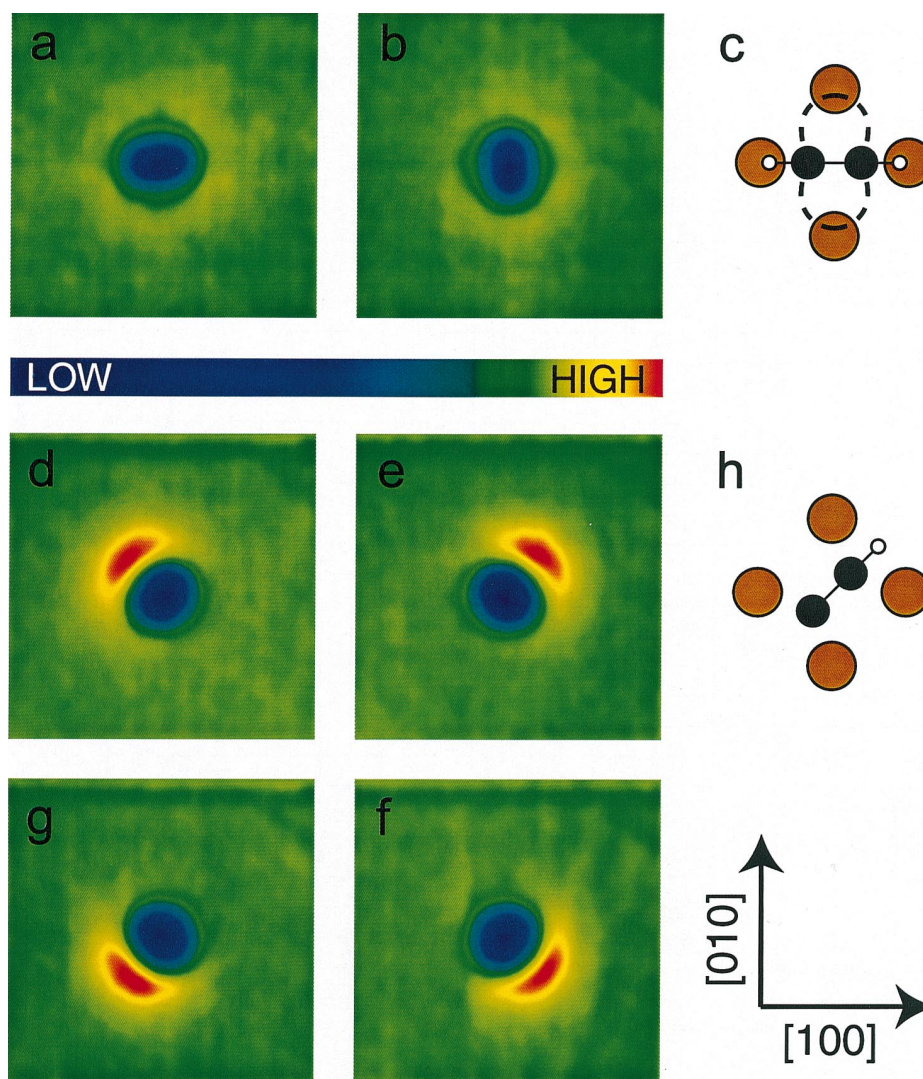*E-mail address:* wilsonho@ccmr.cornell.edu (W. Ho).

Fig. 1. 38 × 38 Å constant current STM images of DCCD and CCD. The tunneling current was 10 pA, the sample bias 50 mV, and the temperature 9 K. The color palette has been adjusted to emphasize structure above the copper plane (green). (a), (b) Two possible orientations of DCCD. (c) Schematic of the DCCD adsorption site of image (b), with the copper atoms shown in color. The scale is magnified 5× with respect to the STM image. (d)–(g) Four possible orientations of CCD. (h) Suggested orientation of CCD in image (e).

then retracted slightly such that a tunneling current of 1 nA resulted when the sample bias was increased to the threshold of 2.8 V[1]. The voltage pulse was terminated upon detection of the slight current increase associated with dissociation of a single C—H bond[2]. The same process was performed on DCCD at a threshold bias of 3.9 V to remove a single D atom. The H(or D) atom was imaged as a small depression in the copper surface. Images of the remaining CCD fragment are shown

_____

[1] The threshold is defined here as the lowest observed bias at which dissociation happens, on average, within 10 s at 1 nA.

[2] The current increases due to a shift of the CCH minimum away from the HCCH minimum.

in Fig. 1d–h. The remaining H(D) of the CCH(CCD) could be removed at a bias of 2.1 V(2.7 V), resulting in a large drop in tunneling current. The CC end-product imaged as a slightly oval depression centered on the same site as the parent acetylene and is not shown here. Individual carbon atoms were not resolved.

Large isotopic differences were seen in the dissociation thresholds of HCCH and CCH. Related effects have been observed in the STM-induced desorption yield of H and D from the Si(100) surface [5] and can be understood by examining the role of mass in the dynamical evolution of the excited state (see, for example, Ref. [6]). Deuterium, being more massive than hydrogen, moves more slowly on the excited state potential energy surface, and is therefore less likely to acquire the energy necessary for desorption. In addition, if the excited state is repulsive, deuterium spends more time closer to the surface and is therefore more effectively quenched due to increased coupling to the surface. In acetylene, the conversion of potential energy to motion along the C−H reaction coordinate is limited by competing relaxation processes. The higher dissociation thresholds for DCCD and CCD indicate that higher-energy electrons are needed to ensure that sufficient energy is delivered to the C−D reaction coordinate. This picture is consistent with the dissociation behavior of the mixed isotope HCCD; dissociation at 3 eV results in the formation of CCD. A similar effect has been noted for STM-induced ethylene dehydrogenation on Ni(110); all isomers of $C_2H_2D_2$ dissociate to C_2D_2 [7].

Tunneling electrons of a few electron-volts can induce changes in HCCH besides single H removal. These effects are particularly noticeable ∼0.2 eV below the dissociation threshold where the rate for single H or D removal is negligible. One possible outcome of molecular excitation is diffusion, or desorption followed by readsorption, resulting in a net translation of the HCCH of 3–15 Å. This is a reasonable outcome of excitation with 2.6 eV electrons as the diffusion barrier of HCCH on Cu(001) was recently determined to be 0.53 eV [4]. The transfer of the HCCH from the surface to the tip was also observed. The transfer was confirmed by depositing the HCCH with a negative

voltage pulse on a clean area of the surface and imaging the molecule in its new location. Most interestingly, the simultaneous removal of two H atoms was also observed[3]. The rate for simultaneous removal is evidently larger than the rate for single H removal at 2.6 eV. The effects noted above were seen for DCCD at 3.7 eV. Finally, the dissociation thresholds for both HCCH and DCCD increased by ∼0.8 eV at 45 K, indicating the existence of efficient quenching processes at this temperature. A temperature-dependent desorption yield has been observed for hydrogen on Si(001) [8]. In the present study, it was also found that diffusion was a more likely outcome than dissociation at 45 K.

The ability to create a CCH fragment in a controlled manner gave us the unique opportunity to study the thermal, electronic, and vibrational excitation of this species at the single molecule level. The electron-induced rotation of CCH and CCD was studied using methods described previously [11]. In brief, the tip is held in a fixed position above, but not centered on, the rotating molecule. When the molecule rotates, the current changes due to the change in tunneling probability. The lifetimes of the molecule in a particular orientation are extracted from the current traces taken for a large number of events. Fig. 2 shows the tunneling electron induced rotation rates of CCH and CCD as a function of sample bias for a fixed tunneling current. A clear threshold is evident in the data, with a similar onset of rotation for both species. The rotation rate was non-linear in the current at 40 mV and linear in the current above 65 mV, indicating the onset of a single electron excitation mechanism.

To elucidate the origin of this behavior, the rotation rates due to thermal excitation CCH and CCD were studied. The rotation rates from 27 to 35.5 K were determined and fit to an Arrhenius law to extract an energy barrier and exponential prefactor. Fits to the data in Fig. 3 give an energy barrier of 56.2 meV (56.8 meV) and a prefactor of $10^{11.0\pm0.1}$ s^{-1} ($10^{10.9\pm0.1}$ s^{-1}) for CCH (CCD).

---

[3] The loss is simultaneous within the time resolution of our electronics. The current is sampled every 20 μs and the rise time of the preamplifier is 250 μs.
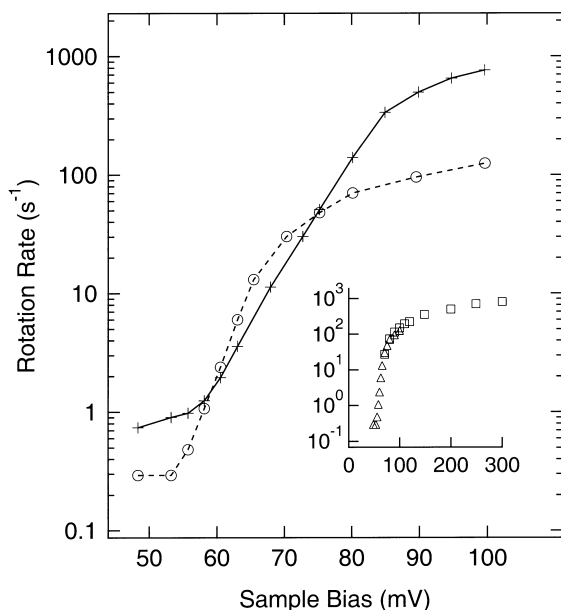
Fig. 2. CCH(+) and CCD(○) rotation rate as a function of the bias voltage at 100 pA. The inset shows data for CCD over a larger bias range taken on two separate occasions. Units for the inset axes are the same as those of the larger graph. Data were taken at 9.5 K.
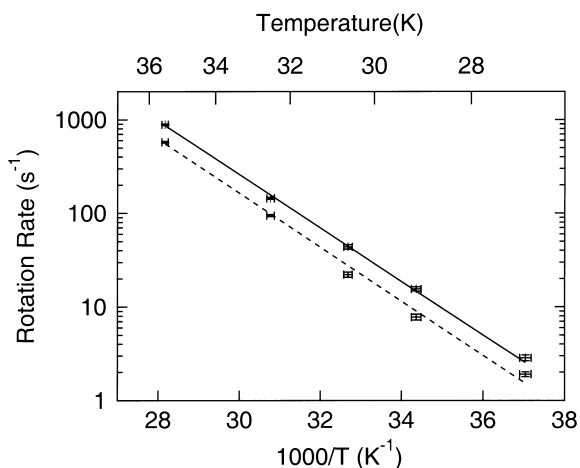

Fig. 3. CCH and CCD rotation rates as a function of temperature. Horizontal error bars are ± 0.1 K. Rotation rates above 30 K were measured at 100 pA and 50 mV. Rotation rates below 30 K were measured using a bias of 24 mV to minimize electron induced rotation. The solid (CCH) and dashed (CCD) lines are fits to an Arrhenius law, $R_r = \nu_r \exp(-E_r/kT)$. The results of the fit are: $E_H = 56.2 \pm 0.5$ meV; $\nu_H = 10^{11.0 \pm 0.1}$ s^{-1}; $E_D = 56.8 \pm 0.5$ meV; $\nu_D = 10^{10.9 \pm 0.1}$ s^{-1}.

The CCD rotation rate at a given temperature was consistently lower than CCH, as was the case for the thermal rotation rate of DCCD compared to that of HCCH [4].

The rotational barrier, combined with the rate-crossing behavior seen in Fig. 2, suggests a mechanism for the electron-induced rotation. The hindered rotational mode of the molecule needs to be excited to overcome the 56 meV rotation barrier. The rotational mode is either directly excited by inelastic scattering events or excited indirectly when higher energy vibrational modes to which it is coupled are excited by inelastic tunneling electrons. The CCD rotation rate exceeds that of CCH because the energy of the relevant vibrational mode is lower and hence excited at lower energies. Once the excitation energy is much larger than the threshold for vibrational excitation, the difference in thresholds becomes irrelevant; the CCH rate becomes larger than the CCD rotation rate due to the larger inelastic tunneling cross-section for H-related modes[4]. The lowest intramolecular vibration for HCCH on Cu(001) was measured by electron energy loss spectroscopy (EELS) to be a CH bending mode at 78 meV [9]. A CH bending mode of CCH was observed at 84 meV in the present study, as described below. The onset of molecular rotation due to a coupling between the bending mode and the hindered rotation is excluded by the observed linear variation of rotation rate with current for 65 meV tunneling electrons. The CCH ν(CM) mode, however, is within a few millielectron-volts of the rotational barrier on several metal surfaces [10], and is therefore a more likely candidate for activating the rotation. Such a coupling is physically plausible since the rotation of the molecule will involve some degree of vertical translation. Typical isotopic differences in energy for the ν(CM) mode are 2–8 meV. The explanation provided above holds for the electron-induced rotation of HCCH and DCCD on Cu(001) [11]. The rotational barrier of 0.17 eV is overcome by exciting the C−H(C−D) stretch mode at 357 meV (265 meV),

---

[4] For all the vibrational modes of various molecules observed to date, the inelastic tunneling cross-section decreases as the isotope mass increases.

which then redistributes its energy to lower lying modes, including the hindered rotation. A similar rate-crossing behavior is seen because the DCCD rotation is 'activated' at a lower energy than the HCCH rotation.

Single-molecule vibrational spectroscopy was performed on CCH and CCD by the recently demonstrated technique of inelastic electron tunneling spectroscopy with the STM (STM-IETS) [3,11,18]. A peak at 395 meV (313 meV) was observed for the CCH(CCD) fragment, which is considerably higher than the 357 meV (265 meV) $C-H(C-D)$ stretch energy of the parent HCCH(DCCD). For comparison, an EELS study of the thermal decomposition products of HCCH on Cu(001) assigned an energy loss at 375 meV to excitation of the $C-H$ stretch of the CCH species [9]. The creation of CCH_2, however, could not be ruled out. In the present study, the spectrum of the HCCD dissociation product was the same as that of the DCCD dissociation product, eliminating the possibility of CCD_2 formation. Because the $C-H$ stretch energy is related to the $C-C$ bond order, experimental determinations of $\nu(CH)$ provide a useful input for theoretical calculations of the interaction of CCH with the Cu(001) surface. A CH(CD) bending mode at 84 meV (63 meV) was also observed by STM-IETS. The peak positions of the $\nu(CH)$ (395 meV) and $\delta(CH)$ (84 meV) modes compare favorably with values of 391 and 84 meV, respectively, observed for CCH on organometallic cluster compounds [10].

Pyridine, benzene, and their fully deuterated isotopes were also studied on Cu(001) at 9 K. Pyridine bonds to a single copper atom through the nitrogen atom and is probably perpendicular to the surface [12], whereas benzene adsorbs more weakly with the molecular plane parallel to the surface [13]. Both molecules image as protrusions on the Cu(001) surface. Pyridine (pyridine-d_5) could be dissociated by 3.0 eV (3.2 eV) electrons, and benzene (benzene-d_6) could be dissociated by 2.9 eV (4.4 eV) electrons. In each case, the dissociation consistently resulted in a single fragment that imaged as a protrusion of distinct symmetry from the parent. Detailed studies of pyridine and benzene dissociation [14] led to the conclusion

that $C-H$ and $C-D$ bonds were being broken in the process and to the suggested fragment identities shown in Fig. 4a and b.

The isotopic difference in dissociation threshold is much greater for benzene (1.5 V) than for pyridine (0.2 V), indicating a different dissociation mechanism. Comparison with thermal and photon-induced dissociation is informative. The photodissociation of benzene at 193 nm results in the removal of one or two H atoms in 96% of events [15]. Likewise, we have argued [14] that the electron-induced dissociation of the weakly adsorbed benzene also results in hydrogen removal. The photodissociation of pyridine at 193 nm results in H removal in only 9% of events; the rest of the events result in destruction of the ring structure. In contrast, the thermal dissociation of pyridine on many metal surfaces results in removal of the α-H, and we have argued that electron-induced dissociation produces the same result. The many degrees of freedom inherent in such large molecules make modeling of the excited state evolution prohibitively complicated, but the experiments described here begin to shed light on the problem. We can say that it is the nature of the pyridine–metal interaction to make α-H bond cleavage facile and to minimize the differences in the excited state evolution of the isotopes, at least with respect to the pathway that leads to dissociation. The weak benzene surface interaction, in contrast, may preserve the gas-phase dissociation mechanism activated by photons.

A large variation in the cross-section for inelastic electron tunneling for pyridine, benzene, and their dissociation products can be seen in the STM-IETS spectra of Fig. 4. Pyridine and the pyridine fragment both exhibit $C-H$ stretch modes, the assignment of which was confirmed by isotopic substitution. It should be noted that multiple $C-H$ stretch modes exist and may contribute to the peak width [14]. The similarity of the parent and fragment spectra suggests that the fragment retains $C-H$ bonds and does not differ radically from the parent[5]. In contrast, benzene does not show

---

[5] The $C-H(C-D)$ peak is upshifted 3 meV (1 meV), in qualitative agreement with spectra for the proposed reaction product. See Ref. [14].
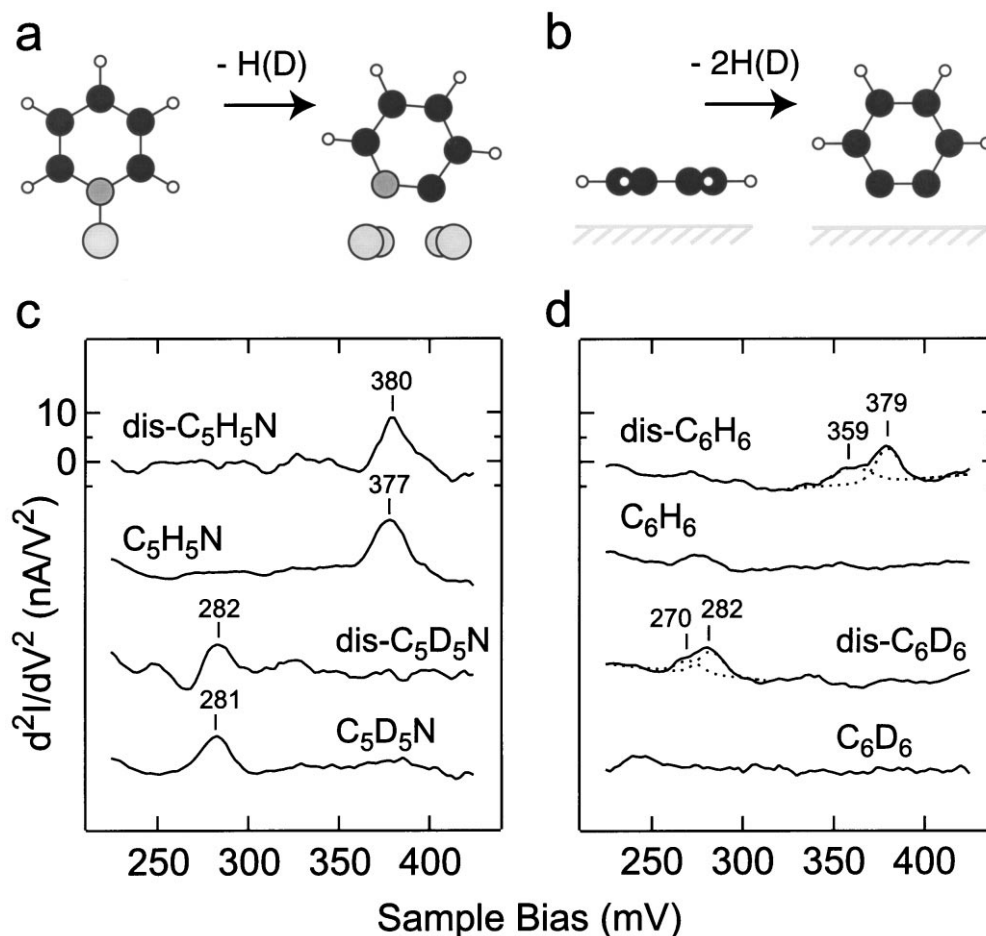
Fig. 4. Proposed transformation of pyridine and benzene via electron-induced dissociation and the effect on the vibrational spectra. A spectrum taken over the bare copper surface has been subtracted from the spectra taken over the molecules. (a) Proposed dissociation reaction for C_5H_5N (C_5D_5N). (b) Proposed dissociation reaction for C_6H_6 (C_6D_6). (c) STM-IETS spectra for C_5H_5N and C_5D_5N compared with their dissociation products. The parent and fragment spectra are averages of 165 and 40 scans, respectively, of 1 min duration. (d) STM-IETS spectra for C_6H_6 and C_6D_6 compared with their dissociation products. The spectra are averages of 100 scans of 1 min duration. For all spectra, the tunneling current was 1 nA at 0.25 V bias and the bias increment 2.5 mV. The a.c. modulation was 7 mV at 200 Hz. Peak assignments were based on the assumption of one tunneling-active mode for pyridine and its fragment and two tunneling-active modes for the benzene fragment.

the existence of C—H stretch modes, yet the dissociation product does. The benzene fragment spectra were best fit by assuming assuming two tunneling-active modes. The onset of C—H stretch modes may be due to the chemical changes induced by hydrogen loss and the subsequent rebonding to the surface. STM-IETS theories have focused on the relative energies of the Fermi level, the molecular electronic resonance, and the molecular vibra-

tion [16,17] but cannot yet be considered predictive. Another possiblity is that the orientation change is primarily responsible for the increased inelastic tunneling. This would imply the existence of selection rules that are well known for more established spectroscopic techniques. The present results, as well as the recent observation of two 'tunneling-active' modes of very different symmetry and energy for CO on Cu(001) [2],

should lead to the development of a more complete theory of STM-IETS. Even in the absence of such a theory, the experimental determination of inelastic tunneling cross-sections can reveal coupling between electronic and vibrational excitations in an adsorbate–surface system.

The understanding of the various phenomena described here is advanced by addressing the question: how is the energy inherent in a non-equilibrium electron distribution channeled into the energy of nuclear motion, that is, how does the injection of tunneling electrons into a molecule result in dissociation, desorption, diffusion, or vibrational excitation? The STM is proving to be a very useful tool in answering this long-standing question by providing a window on the molecule's exploration of its excited state potential energy surface. This exploration is a critical component of chemical transformation.

Acknowledgement

References

[1] B.C. Stipe, M.A. Rezaei, W. Ho, Rev. Sci. Instrum. 70 (1999) 137.
[2] L.J. Lauhon, W. Ho, Phys. Rev. B 60 (1999) R8525.
[3] B.C. Stipe, M.A. Rezaei, W. Ho, Science 280 (1998) 1732.
[4] L.J. Lauhon, W. Ho, J. Chem. Phys. 111 (1999) 5633.
[5] Ph. Avouris, R.E. Walkup, A.R. Rossi, T.-C. Shen, G.C. Abeln, J.R. Tucker, J.W. Lyding, Chem. Phys. Lett. 257 (1996) 148.
[6] R.D. Ramsier, J.T. Yates Jr., Surf. Sci. Rep. 12 (1991) 243.
[7] J. Gaudioso, H.J. Lee, W. Ho, J. Am. Chem. Soc. 121 (1999) 8479.
[8] E.T. Foley, A.F. Kam, J.W. Lyding, Ph. Avouris, Phys. Rev. Lett. 80 (1998) 1336.
[9] Ts.S. Marinova, P.K. Stefanov, Surf. Sci. 191 (1987) 66.
[10] B.E. Koel, J.E. Crowell, B.E. Bent, C.M. Mate, G.A. Somorjai, J. Phys. Chem. 90 (1986) 2949.
[11] B.C. Stipe, M.A. Rezaei, W. Ho, Phys. Rev. Lett. 81 (1998) 1263.
[12] M.E. Bridge, M. Connolly, D.R. Lloyd, J. Somers, P. Jakob, D. Menzel, Spec. Chim. Acta A 43 (1987) 1473.
[13] L. Triguero, L.G.M. Pettersson, B. Minaev, H. Agren, J. Chem. Phys. 108 (1998) 1193.
[14] L.J. Lauhon, W. Ho, J. Phys. Chem. (2000) in press.
[15] K.A. Prather, Y.T. Lee, Isr. J. Chem. 34 (1994) 43.
[16] B.N.J. Persson, A. Baratoff, Phys. Rev. Lett. 59 (1987) 339.
[17] M.A. Gata, P.R. Antoniewicz, Phys. Rev. B 47 (1993) 13 797.
[18] L.J. Lauhon, W. Ho, Phys. Rev. Lett. 84 (2000) 1527.